

Quantum Geometric Origin of Hall Viscosity and Nonlocal Hall Conductivity in Lattice Bands

Danyu Shu,^{1,*} Ryotaro Sano,² Ai Yamakage,³ Hiroshi Funaki,⁴ and Mamoru Matsuo^{1,5,6,7,†}

¹*Kavli Institute for Theoretical Sciences, University of Chinese Academy of Sciences, Beijing, 100190, China.*

²*Institute of Solid State Physics, University of Tokyo, Kashiwa 277-8581, Japan*

³*Department of Physics, Nagoya University, Nagoya 464-8602, Japan*

⁴*Center for Spintronics Research Network, Keio University, Yokohama 223-8522, Japan*

⁵*CAS Center for Excellence in Topological Quantum Computation, University of Chinese Academy of Sciences, Beijing 100190, China*

⁶*RIKEN Center for Emergent Matter Science (CEMS), Wako, Saitama 351-0198, Japan*

⁷*Advanced Science Research Center, Japan Atomic Energy Agency, Tokai, 319-1195, Japan*

(Dated: May 27, 2026)

We show that Hall viscosity in lattice bands is governed by a band-projected electric quadrupole encoded within the quantum geometry: Berry curvature sets the projected-coordinate algebra, while the quantum metric determines the quadrupolar spread of a wave packet. The same structure enters the quadratic wave-vector coefficient of the nonlocal Hall conductivity, yielding a lattice viscosity-conductivity relation. In ideal bands, the deviation from the Landau-level form is quantified by Berry curvature fluctuations. Our results establish the nonlocal Hall response as an electrical signature of the quantum geometry underlying Hall viscosity and as a transport diagnostic of geometric idealness.

Introduction— Recent experimental realizations of Chern bands and moiré flat bands have elevated quantum geometry to a central organizing concept in crystalline quantum matter [1–7]. In ideal or nearly ideal Chern bands, Berry curvature and the quantum metric control how closely a lattice band mimics a Landau level [8–23] and thereby affect the stability of correlated topological phases [24–26]. A key challenge is to identify measurable responses that reflect the relevant quantum geometry. Among such responses, Hall viscosity is a canonical nondissipative response to dynamical strain, encoding the internal geometry of topological fluids [27–31]. However, direct measurement of Hall viscosity in crystalline systems remains difficult because it requires coupling to mechanical deformation, although indirect electrical detection has been demonstrated in the hydrodynamic regime of graphene [32]. It is therefore desirable to identify an electrical observable that captures the same band-geometric content in gapped Bloch bands.

Haldane’s electric-quadrupole picture of quantum Hall fluids provides a natural route to establish this connection [33, 34]. In this formulation, the Hall-viscous response is encoded in a primitive electric quadrupole built from the guiding-center coordinates within a Landau level. Because such a quadrupole couples to gradients of a spatially nonuniform electric field, it can be electrically accessed through the nonlocal Hall response [35–41]. In a continuum Landau level, the noncommutative guiding-center algebra and the magnetic length are intrinsic to the underlying kinematics [42–44]. By contrast, lattice bands have no such built-in guiding-center structure. This absence calls for a reconstruction of the relevant quadrupole from the band-projected position operator, thereby recasting the electric-quadrupole picture in terms of Bloch-band quantum geometry.

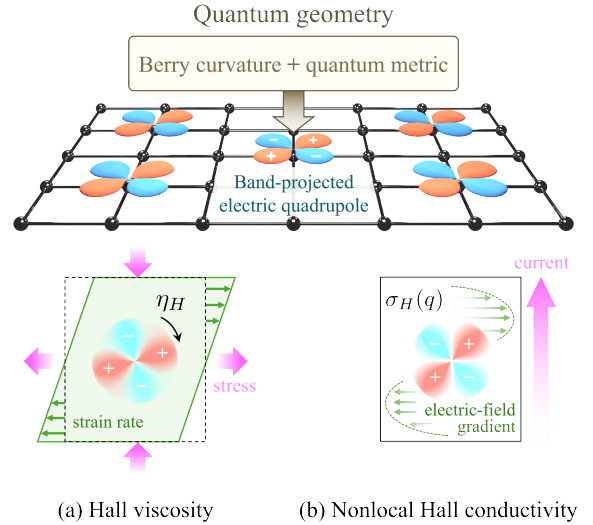


FIG. 1. Conceptual schematic of the geometric quadrupole picture. The quantum metric and Berry curvature define the band-projected electric quadrupole, which underlies (a) the Hall viscous response to dynamical strain and (b) the nonlocal Hall response to a spatially nonuniform electric field. Green and pink arrows in the lower panels indicate the applied perturbations and induced Hall responses, respectively.

In this Letter, we carry out this reconstruction within an isolated Bloch band without invoking the kinematics of a continuum Landau level (see Fig. 1). Projecting the position operator itself generates the lattice analogue of the guiding center, with its noncommutative algebra set by Berry curvature and the intrinsic quadrupole of a semiclassical wave packet determined by the quantum metric. Since these two quantities are the imaginary and real parts of the quantum geometric tensor (QGT) [45–

[48], the resulting band-projected quadrupole provides a microscopic geometric variable underlying Hall viscosity in lattice bands. Specifically, quantum geometric inequalities set a lower bound on the isotropic component [49, 50]. We further show that this projected quadrupole enters the quadratic wave-vector coefficient of the nonlocal Hall conductivity. This yields a lattice viscosity-conductivity relation rooted in projected band geometry. In generic nonideal bands, the relation contains lattice corrections governed by correlations between the quantum metric and Berry curvature. In ideal bands satisfying the trace condition [13, 16], these corrections simplify, and the remaining deviation from the Landau-level form is controlled by Berry-curvature fluctuations. This establishes the quadratic nonlocal Hall response as an electrical signature of the band-projected quantum geometry and as a diagnostic of geometric idealness relevant to the stability of fractional Chern insulating phases.

Viscosity tensor and Hall viscosity— We first express dissipationless viscosity as an equal-time commutator of strain generators. The viscosity tensor $\eta_{\mu\nu\alpha\beta}$ is defined as the response of the stress tensor $\langle \hat{T}_{\mu\nu} \rangle$ to the strain rate $\dot{\lambda}_{\alpha\beta}$ [27, 28]

$$\langle \hat{T}_{\mu\nu} \rangle = -\eta_{\mu\nu\alpha\beta} \frac{\partial \lambda_{\alpha\beta}}{\partial t}. \quad (1)$$

According to standard fluid mechanics [51], the rate of energy dissipation is $\dot{\epsilon} = \langle \hat{T}_{\mu\nu} \rangle \dot{\lambda}_{\mu\nu}$, and dissipationless Hall viscosity is the part antisymmetric under the exchange of index pairs $\mu\nu \leftrightarrow \alpha\beta$. In quantum mechanics, uniform strain transformations are described by the d -dimensional general linear group $\text{GL}(d, \mathbb{R})$ [37]. The generator of strain deformation $\hat{J}_{\mu\nu}$ is defined by

$$[\hat{J}_{\mu\nu}, \hat{x}_\alpha] = i\hbar \delta_{\alpha\nu} \hat{x}_\mu, \quad (2)$$

and the stress tensor is its time derivative, $\hat{T}_{\mu\nu} \equiv -\partial_t \hat{J}_{\mu\nu}$. To calculate $\eta_{\mu\nu\alpha\beta}$ from a Kubo formula [37, 52, 53], we first specify the perturbation. Analogous to the length ($H' = -e\mathbf{E} \cdot \hat{\mathbf{x}}$) and velocity gauges ($H' = -e\mathbf{A} \cdot \hat{\mathbf{v}}$) in conductivity calculations, strain admits two gauge choices, $H' = -\dot{\lambda}_{\mu\nu} \hat{J}_{\mu\nu}$ and $H' = -\dot{\lambda}_{\mu\nu} \hat{T}_{\mu\nu}$. We use the former, which yields the static viscosity [54]

$$\eta_{\mu\nu\alpha\beta}(\omega \rightarrow 0) = -\frac{i}{\hbar} \langle [\hat{J}_{\mu\nu}, \hat{J}_{\alpha\beta}] \rangle_0, \quad (3)$$

which is dissipationless by construction. By analogy with the Berry-curvature formula for Hall conductivity, η_H can be written in terms of Berry curvature in strain space $\lambda_{\mu\nu}$ [27]. In the following, we instead extend Eq. (3) to lattice systems and express Hall viscosity through the quantum metric and Berry curvature in reciprocal space.

Quadrupole response and quantum geometric formula of Hall viscosity— We now construct the band-projected strain generator from the electric quadrupole and connect it to the quantum geometry. Haldane has formulated the quantum Hall state as an incompressible fluid

characterized by a primitive electric quadrupole [34], requiring only inversion symmetry rather than continuous rotational symmetry. This is achieved by decomposing the position operator $\hat{\mathbf{x}}$ into guiding-center and relative orbital motion [33, 55], and applying the same decomposition to the electric quadrupole.

To construct the lattice counterpart of this guiding-center decomposition, we start from the position operator in the Bloch basis. The matrix elements of $\hat{\mathbf{x}}$ between Bloch states $|\psi_n(\mathbf{k})\rangle = e^{i\mathbf{k} \cdot \hat{\mathbf{x}}} |u_n(\mathbf{k})\rangle$ are $\langle \psi_n(\mathbf{k}) | \hat{\mathbf{x}} | \psi_m(\mathbf{k}') \rangle = [\delta_{nm} i \nabla_{\mathbf{k}} + \mathbf{A}_{nm}(\mathbf{k})] \delta(\mathbf{k} - \mathbf{k}')$, where $\mathbf{A}_{nm}(\mathbf{k}) \equiv i \langle u_n(\mathbf{k}) | \nabla_{\mathbf{k}} | u_m(\mathbf{k}) \rangle$ is the non-Abelian Berry connection [56]. Thus, the lattice analogue of the guiding-center coordinates is obtained by projecting $\hat{\mathbf{x}}$ onto an isolated band. The remaining interband matrix elements encode the intrinsic orbital spread of a wave packet and give rise to the quantum metric.

In the adiabatic regime, where the relevant energy scales of the external perturbations are sufficiently weak compared with the gap to other bands, interband mixing can be safely neglected. Projecting the position operator onto an isolated single-band subspace, then yields the covariant coordinate $\hat{\mathbf{X}} = i \nabla_{\mathbf{k}} + \mathbf{A}(\mathbf{k})$, where band indices are omitted for brevity and $\mathbf{A}(\mathbf{k})$ denotes the Berry connection.

In close analogy with guiding-center coordinates in a Landau level, the band-projected coordinates obey a non-commutative coordinate algebra,

$$[\hat{X}_\mu, \hat{X}_\nu] = i \Omega_{\mu\nu}(\mathbf{k}), \quad (4)$$

where $\Omega_{\mu\nu}(\mathbf{k}) = \partial_\mu A_\nu(\mathbf{k}) - \partial_\nu A_\mu(\mathbf{k})$ is the Berry curvature. This algebra is the lattice counterpart of the guiding-center algebra.

We further define the primitive electric quadrupole as $\hat{Q}_{\mu\nu} \equiv \frac{1}{2} \{ \hat{X}_\mu, \hat{X}_\nu \} - \langle \hat{X}_\mu \rangle \langle \hat{X}_\nu \rangle$, where $\langle \dots \rangle$ denotes the expectation value evaluated over the generic localized quantum state under consideration. From the nontrivial commutator of the projected position operators in Eq. (4), the quadrupole obeys an $\text{SO}(2, 1)$ Lie algebra: $[\hat{Q}_{\mu\nu}, \hat{Q}_{\alpha\beta}] = i \Omega_{\nu\beta} \hat{Q}_{\mu\alpha} + i \Omega_{\mu\beta} \hat{Q}_{\alpha\nu} + (\alpha \leftrightarrow \beta)$.

The strain generator $\hat{J}_{\mu\nu}$ satisfying Eq. (2) is then

$$\hat{J}_{\mu\nu} = \frac{\hbar}{2\Omega} \epsilon_{\nu\lambda} \hat{Q}_{\mu\lambda} + \frac{1}{2} \delta_{\mu\nu} \hat{D}, \quad (5)$$

where $\Omega \equiv \epsilon_{\mu\nu} \Omega_{\mu\nu} / 2$ is the scalar Berry curvature. Because the quadrupole $\hat{Q}_{\mu\nu}$ is symmetric by definition, the first term of Eq. (5) is traceless and contains shears (symmetric parts) and rotations (antisymmetric parts). The operator \hat{D} describes dilation and obeys $[\hat{D}, \hat{X}_\alpha] = i\hbar \hat{X}_\alpha$. The explicit form of \hat{D} involves interband matrix elements and is not necessary if we focus on dissipationless response. To calculate Hall viscosity from Eq. (3), we need

$$\begin{aligned} [\hat{J}_{\mu\nu}, \hat{J}_{\alpha\beta}] &= -i\hbar (\delta_{\mu\beta} \hat{J}_{\alpha\nu} - \delta_{\nu\alpha} \hat{J}_{\mu\beta}) \\ &\quad + i\hbar (\delta_{\mu\nu} \hat{J}_{\alpha\beta} - \delta_{\alpha\beta} \hat{J}_{\mu\nu}), \end{aligned} \quad (6)$$

where the first line is traceless in α, β , whereas the second line is not and therefore involves compressibility. At the level of the bulk viscous force $f_\nu \equiv \eta_{\mu\nu\alpha\beta} \partial_\mu \dot{\lambda}_{\alpha\beta}$, however, these two terms are indistinguishable because only the components symmetric under $\mu \leftrightarrow \alpha$ contribute. They can therefore be separated only through boundary forces or symmetry.

All terms containing \hat{D} cancel in Eq. (6). It then shows how the familiar single Hall viscosity coefficient of a rotationally invariant Landau level is generalized in a lattice band [57]. Since the electric quadrupole $\hat{Q}_{\mu\nu}$ is symmetric, the traceless parts of $\hat{J}_{\mu\nu}$ can be decomposed into the three two-dimensional tensor structures ϵ , σ^x , and σ^z . The Hall-viscosity tensor is antisymmetric and therefore contains six independent components in two dimensions [58]. In the presence of continuous rotational symmetry, the Hall-viscosity tensor reduces to a scalar, $\eta_{\mu\nu\alpha\beta} \propto \eta_H (\delta_{\alpha\nu} \epsilon_{\mu\beta} - \delta_{\mu\beta} \epsilon_{\alpha\nu})$, where η_H is the isotropic Hall viscosity.

The expectation value in Eq. (6) is evaluated within the isolated-band subspace specified above. We use a semiclassical wave packet $|\Psi(t)\rangle = \int d\mathbf{k} a(\mathbf{k}, t) |\psi(\mathbf{k})\rangle$ [59, 60], where $a(\mathbf{k}, t)$ is normalized and sharply peaked around $\mathbf{K}(t)$ in reciprocal space. The position of this wave packet, $\mathbf{X}(t) \equiv \langle \Psi(t) | \hat{\mathbf{x}} | \Psi(t) \rangle = \int d\mathbf{k} a^*(\mathbf{k}, t) [\hat{\mathbf{X}} a(\mathbf{k}, t)]$, identifies $\hat{\mathbf{X}}$ as the wave-packet center of mass, in analogy with the guiding center of a quantum Hall state. Beyond this center-of-mass motion, the intrinsic spatial extent of the wave packet is characterized by its primitive electric quadrupole. By evaluating the spatial variance $\langle \Psi(t) | \hat{x}_\mu \hat{x}_\nu | \Psi(t) \rangle = X_\mu X_\nu + g_{\mu\nu}(\mathbf{K})$, we reveal a rigorous geometric equivalence: $\langle \hat{Q}_{\mu\nu}(\mathbf{K}) \rangle = g_{\mu\nu}(\mathbf{K})$ [61, 62] where $g_{\mu\nu}(\mathbf{k}) \equiv \text{Re} \langle \partial_\mu u(\mathbf{k}) | \partial_\nu u(\mathbf{k}) \rangle - A_\mu(\mathbf{k}) A_\nu(\mathbf{k})$ denotes the quantum metric.

Since $g_{\mu\nu}$ is symmetric, it can be expanded in the basis δ , σ^x , and σ^z . The isotropic Hall viscosity η_H , corresponding to the δ component, is thus given by:

$$\eta_H = -\frac{\hbar}{4} \int_{\text{BZ}} \frac{d^2 \mathbf{k}}{4\pi^2} \frac{\text{tr}[g(\mathbf{k})]}{\Omega(\mathbf{k})}. \quad (7)$$

Other components follow in the same way by replacing $\text{tr}[g]$ with $\sigma_{\mu\nu}^x g_{\mu\nu}$ or $\sigma_{\mu\nu}^z g_{\mu\nu}$. This formulation differs from previous lattice approaches based on Berry-curvature moments [57], because Hall viscosity is determined by the full QGT rather than by Berry-curvature moments alone.

Time-reversal symmetry imposes $g_{\mu\nu}(\mathbf{k}) = g_{\mu\nu}(-\mathbf{k})$ and $\Omega(\mathbf{k}) = -\Omega(-\mathbf{k})$. Under this condition, the Chern number C , which characterizes the Hall conductivity, vanishes, and each Hall-viscosity component vanishes. This is consistent with the dissipationless nature of Hall viscosity and points to a connection with nonlocal Hall conductivity.

As a benchmark, we consider the rotationally invariant continuum limit of the IQHE. When the underlying

lattice constant is much smaller than the magnetic length $l_B = \sqrt{\hbar/eB}$, the quantum geometry of an occupied n -th Landau level is uniform across the Brillouin zone: the quantum metric and Berry curvature take the forms $g_{\mu\nu} = \delta_{\mu\nu} l_B^2 (n + 1/2)$ and $\Omega_{\mu\nu} = -l_B^2 \epsilon_{\mu\nu}$, respectively [49, 50]. Substitution into Eq. (7) shows that each Landau level contributes $\frac{\hbar}{2} (n + 1/2)$ to the Hall-viscosity density, reproducing the well-established continuum result [27, 63–65].

In generic crystalline lattices, $g_{\mu\nu}(\mathbf{k})$ and $\Omega_{\mu\nu}(\mathbf{k})$ acquire momentum dependence, but their local relation: $\text{tr}[g(\mathbf{k})] \geq 2\sqrt{\det[g(\mathbf{k})]} \geq |\Omega(\mathbf{k})|$ is constrained by the quantum geometric inequality [13, 50]. Integrating this inequality over the Brillouin zone yields a lower bound $\hbar\rho/4$ for the isotropic Hall-viscosity density. A subtlety arises at zeros of Berry curvature, $\Omega(\mathbf{k}) = 0$. At such points the projected position operators commute, and the quadrupolar wave-packet construction becomes trivial. The ideal bands of primary interest avoid this singular case because the trace condition constrains the Bloch wave functions to be holomorphic or antiholomorphic in $k_x \pm ik_y$, and the Berry curvature has a definite sign throughout the Brillouin zone.

Viscosity-conductivity relation— Furthermore, the intrinsic electric quadrupole fundamentally also governs the quadratic wave-vector coefficient (q^2) of the nonlocal Hall conductivity, arising from the quantum state's response to a spatially nonuniform electric field $\mathbf{E}(\mathbf{x})$. Because both Hall viscosity and this second-order transport coefficient share a common microscopic geometric origin, we are naturally led to anticipate a direct connection between them. Indeed, in continuous Galilean-invariant systems, this intrinsic link manifests as a well-established universal relation. For the IQHE [36, 66], the second-order nonlocal Hall conductivity $\sigma_H^{(2)}(\mathbf{q})$ is strictly proportional to the Hall viscosity:

$$\sigma_H^{(2)}(\mathbf{q}) = \sigma_H^{(0)} \cdot \frac{\eta_H}{\rho \hbar} \cdot (ql_B)^2, \quad (8)$$

where $\rho = N_L/2\pi l_B^2$ is the electron density and N_L is the Landau-level occupation number. In a crystal, velocity differs from momentum due to the absence of Galilean invariance. Consequently, no general relation between viscosity and conductivity is guaranteed. Our result identifies the remaining correlation and quantifies its deviation by Berry-curvature fluctuations.

At leading order in the electric-field gradient and within the adiabatic single-band approximation, the nonlocal Hall response is captured by the semiclassical wave-packet dynamics. Under a nonuniform electric field, the equation of motion for the wave-packet center remains $\dot{X}_\mu = \hbar^{-1} \partial \epsilon / \partial K_\mu - \Omega_{\mu\nu} \dot{K}_\nu$, while that for the momentum becomes $\dot{K}_\mu = -e [E_\mu + \frac{1}{2} g_{\alpha\beta}(\mathbf{K}) \partial_\alpha \partial_\beta E_\mu]$ [61, 62].

For an insulating system where the chemical potential lies strictly within the bulk band gap, the second term yields the second-order nonlocal Hall conductivity:

$$\sigma_H^{(2)}(\mathbf{q}) = \frac{e^2}{\hbar} \int_{\text{BZ}} \frac{d^2\mathbf{k}}{4\pi^2} \frac{1}{2} g_{\alpha\beta}(\mathbf{k}) \Omega(\mathbf{k}) q_\alpha q_\beta. \quad (9)$$

To formulate the viscosity-conductivity relation on a lattice, one needs a length scale playing the role of the magnetic length l_B . In a quantum Hall state, $2\pi l_B^2$ is the minimal area occupied by an electron due to the Heisenberg uncertainty principle. In a Bloch band, the fundamental lower bound for the spatial spread of bulk wave packets, saturated by maximally localized Wannier functions, is rigorously governed by $\text{tr}[g(\mathbf{k})]$ [67, 68]. Furthermore, recent studies have demonstrated that the spatial penetration depth of topological boundary modes is also intimately tied to this exact quantum metric length [69]. This geometric correspondence naturally motivates replacing $(ql_B)^2$ by $g_{\alpha\beta}q_\alpha q_\beta$.

Guided by this geometric interpretation of the characteristic length, we can now systematically re-evaluate the full lattice response in Eq. (9). To explicitly separate the uniform topological contribution from the effects of local geometric variations, it is highly instructive to perform a statistical decomposition over the Brillouin zone:

$$\sigma_H^{(2)}(\mathbf{q}) = \frac{e^2}{\hbar} q_\alpha q_\beta \left[\frac{C}{2} \langle g_{\alpha\beta} \rangle_{\text{BZ}} + \frac{A_{\text{BZ}}}{4\pi} \text{Cov}(g_{\alpha\beta}, \Omega) \right], \quad (10)$$

where $\langle \dots \rangle_{\text{BZ}} \equiv \int_{\text{BZ}} d^2\mathbf{k} (\dots) / A_{\text{BZ}}$ denotes the Brillouin-zone average, A_{BZ} is the area of the first Brillouin zone, $\langle \Omega \rangle_{\text{BZ}} = 2\pi C / A_{\text{BZ}}$, and $\text{Cov}(f, g) \equiv \langle f \cdot g \rangle_{\text{BZ}} - \langle f \rangle_{\text{BZ}} \langle g \rangle_{\text{BZ}}$.

The first term averages over microscopic lattice details and captures the contribution of a uniform topological background, matching the continuous lowest-Landau-level (LLL) limit where local geometric fluctuations are absent. The second term measures the correlation between the quantum metric and Berry curvature, quantified by their covariance over the Brillouin zone.

To relate the nonlocal Hall conductivity $\sigma_H^{(2)}(\mathbf{q})$ in Eq. (9) and the isotropic Hall viscosity η_H in Eq. (7), we focus on the q^2 term and adopt the decomposition

$$\sigma_H^{(2)}(\mathbf{q}) = \frac{e^2}{\hbar} q^2 \frac{A_{\text{BZ}}}{8\pi} \left[\left\langle \frac{\text{tr}[g]}{\Omega} \right\rangle_{\text{BZ}} \langle \Omega^2 \rangle_{\text{BZ}} + \text{Cov}\left(\frac{\text{tr}[g]}{\Omega}, \Omega^2\right) \right]. \quad (11)$$

While Eq. (10) displays the generic lattice correction as a metric-curvature covariance, Eq. (11) reorganizes the same response with the factor entering Hall viscosity, $\langle \text{tr}[g]/\Omega \rangle_{\text{BZ}}$, made more explicit. For an ideal band satisfying the trace condition $\text{tr}[g(\mathbf{k})] = |\Omega(\mathbf{k})|$ [13], and with Berry curvature of a definite sign throughout the Brillouin zone, the covariance term vanishes even if the Berry curvature is not constant and Eq. (11) reduces to

$$\sigma_H^{(2)}(\mathbf{q}) = \sigma_H^{(0)} \cdot \frac{\eta_H}{\rho \hbar} \cdot q^2 \langle -\Omega \rangle_{\text{BZ}} \cdot (1 + F_\Omega^2), \quad (12)$$

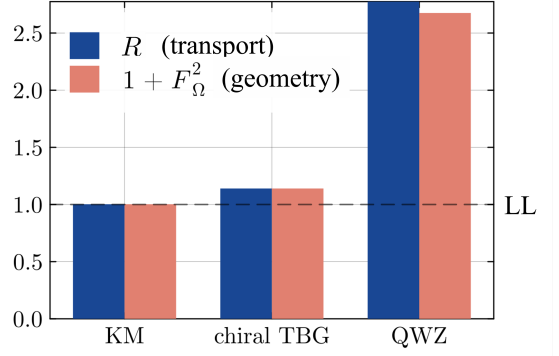


FIG. 2. Transport signature of geometric idealness. The non-local Hall ratio R is compared with the ideal-band expression $1 + F_\Omega^2$ for three representative Chern bands: Kapit–Mueller (KM), chiral twisted bilayer graphene (chiral TBG), and Qi–Wu–Zhang (QWZ) models. The dashed line denotes the Landau-level (LL) benchmark $R = 1$, corresponding to the ideal-band limit with uniform Berry curvature.

where $\sigma_H^{(0)} = Ce^2/h$ is the uniform Hall conductivity and $\rho = A_{\text{BZ}}/4\pi^2$ is the electron density. Here, l_B^2 in Eq. (8) is replaced by $\langle -\Omega \rangle_{\text{BZ}} (1 + F_\Omega^2)$. In such systems, the deviation from the Landau-level relation in Eq. (8) is thus simply quantified by the dimensionless Berry-curvature fluctuation F_Ω over the Brillouin zone:

$$F_\Omega \equiv \sqrt{\int_{\text{BZ}} \frac{d^2\mathbf{k}}{A_{\text{BZ}}} \left[\frac{\Omega(\mathbf{k})}{2\pi C / A_{\text{BZ}}} - 1 \right]^2}. \quad (13)$$

To recast the above relation in terms of experimental observables without using microscopic wave-function data, we introduce the dimensionless nonlocal Hall ratio,

$$R = \frac{4\pi\rho}{|\nu_H|} \left. \frac{\partial^2}{\partial q^2} \ln |\sigma_H(\mathbf{q})| \right|_{q=0}, \quad (14)$$

where $\nu_H \equiv \sigma_H^{(0)} / (e^2/h)$ is the normalized uniform Hall conductivity obtained from the measured $\mathbf{q} = 0$ response. For a filled isolated Chern band, $\nu_H = C$. The ratio R is therefore determined from experimental inputs alone, rather than from microscopic band-geometric data. For a sign-definite band satisfying the trace condition, it reduces to $1 + F_\Omega^2$, and further to the Landau-level value $R = 1$ when Berry curvature is uniform over the Brillouin zone.

We then evaluate R for representative Chern bands and compare it with the ideal-band expression $1 + F_\Omega^2$, where F_Ω is computed from the Berry-curvature distribution [70]. The Kapit–Mueller (KM) model with long-range hopping serves as a nearly Landau-level reference [12, 71], chiral twisted bilayer graphene (chiral TBG) in the continuum limit provides an example of a moiré Chern band [15, 16, 20], and the Qi–Wu–Zhang (QWZ) model represents a generic nonideal Chern band [72]. As shown in Fig. 2, R is pinned close

to the Landau-level value for the KM band, is moderately enhanced in chiral TBG reflecting finite Berry-curvature fluctuations, and is substantially larger in the QWZ model. Agreement between R and $1 + F_{\Omega}^2$ indicates that the band geometry realizes the trace-condition ideal limit. Within this ideal class, the deviation of R from unity measures Berry-curvature fluctuations over the Brillouin zone. Thus, the nonlocal Hall ratio acts as a transport diagnostic of geometric idealness.

Conclusions— We have identified the band-projected electric quadrupole as the microscopic variable that realizes Haldane’s quadrupole picture in an isolated Bloch band. The band-projected coordinate supplies the guiding-center kinematics, Berry curvature fixes its commutator, and the quantum metric determines the intrinsic quadrupole carried by a semiclassical wave packet. This construction yields the projected-band contribution to the antisymmetric viscosity tensor in lattice bands. The quantum geometric inequality then gives a lower bound on the isotropic Hall viscosity component. We further showed that the quadratic wave-vector coefficient of the nonlocal Hall conductivity encodes the same projected quadrupole, thereby connecting Hall viscosity to an electrically measurable nonlocal transport coefficient. In this band-projected formulation, the magnetic-length scale in the continuum viscosity-conductivity relation is replaced by Brillouin-zone averages and covariance corrections of the band geometry. Deviations from the Landau-level-like relation then provide an electrical diagnostic of geometric idealness relevant to fractional Chern insulating phases.

* shudanyu24@mails.ucas.ac.cn

† mamoru@ucas.ac.cn

- [1] Jiaqi Cai, Eric Anderson, Chong Wang, Xiaowei Zhang, Xiaoyu Liu, William Holtzmann, Yinong Zhang, Fengren Fan, Takashi Taniguchi, Kenji Watanabe, Ying Ran, Ting Cao, Liang Fu, Di Xiao, Wang Yao, and Xiaodong Xu, “Signatures of fractional quantum anomalous Hall states in twisted MoTe₂,” *Nature* **622**, 63–68 (2023).
- [2] Heonjoon Park, Jiaqi Cai, Eric Anderson, Yinong Zhang, Jiayi Zhu, Xiaoyu Liu, Chong Wang, William Holtzmann, Chaowei Hu, Zhaoyu Liu, Takashi Taniguchi, Kenji Watanabe, Jiun-Haw Chu, Ting Cao, Liang Fu, Wang Yao, Cui-Zu Chang, David Cobden, Di Xiao, and Xiaodong Xu, “Observation of fractionally quantized anomalous Hall effect,” *Nature* **622**, 74–79 (2023).
- [3] Fan Xu, Zheng Sun, Tongtong Jia, Chang Liu, Cheng Xu, Chushan Li, Yu Gu, Kenji Watanabe, Takashi Taniguchi, Bingbing Tong, Jinfeng Jia, Zhiwen Shi, Shengwei Jiang, Yang Zhang, Xiaoxue Liu, and Tingxin Li, “Observation of Integer and Fractional Quantum Anomalous Hall Effects in Twisted Bilayer MoTe₂,” *Physical Review X* **13**, 031037 (2023).
- [4] Zhenguang Lu, Tonghang Han, Yuxuan Yao, Aidan P. Reddy, Jixiang Yang, Junseok Seo, Kenji Watanabe, Takashi Taniguchi, Liang Fu, and Long Ju, “Fractional quantum anomalous Hall effect in multilayer graphene,” *Nature* **626**, 759–764 (2024).
- [5] Zhurun Ji, Heonjoon Park, Mark E. Barber, Chaowei Hu, Kenji Watanabe, Takashi Taniguchi, Jiun-Haw Chu, Xiaodong Xu, and Zhi-Xun Shen, “Local probe of bulk and edge states in a fractional Chern insulator,” *Nature* **635**, 578–583 (2024).
- [6] Evgeny Redekop, Canxun Zhang, Heonjoon Park, Jiaqi Cai, Eric Anderson, Owen Sheekey, Trevor Arp, Grigory Babikyan, Samuel Salters, Kenji Watanabe, Takashi Taniguchi, Martin E. Huber, Xiaodong Xu, and Andrea F. Young, “Direct magnetic imaging of fractional Chern insulators in twisted MoTe₂,” *Nature* **635**, 584–589 (2024).
- [7] Eric Anderson, Jiaqi Cai, Aidan P. Reddy, Heonjoon Park, William Holtzmann, Kai Davis, Takashi Taniguchi, Kenji Watanabe, Tomasz Smolenski, Ataç Imamoğlu, Ting Cao, Di Xiao, Liang Fu, Wang Yao, and Xiaodong Xu, “Trion sensing of a zero-field composite Fermi liquid,” *Nature* **635**, 590–595 (2024).
- [8] Evelyn Tang, Jia-Wei Mei, and Xiao-Gang Wen, “High-Temperature Fractional Quantum Hall States,” *Physical Review Letters* **106**, 236802 (2011).
- [9] Kai Sun, Zhengcheng Gu, Hoshio Katsura, and S. Das Sarma, “Nearly Flatbands with Nontrivial Topology,” *Physical Review Letters* **106**, 236803 (2011).
- [10] N. Regnault and B. Andrei Bernevig, “Fractional Chern Insulator,” *Physical Review X* **1**, 021014 (2011).
- [11] Titus Neupert, Luiz Santos, Claudio Chamon, and Christopher Mudry, “Fractional Quantum Hall States at Zero Magnetic Field,” *Physical Review Letters* **106**, 236804 (2011).
- [12] Eliot Kapit and Erich Mueller, “Exact Parent Hamiltonian for the Quantum Hall States in a Lattice,” *Physical Review Letters* **105**, 215303 (2010).
- [13] Rahul Roy, “Band geometry of fractional topological insulators,” *Physical Review B* **90**, 165139 (2014).
- [14] Martin Claassen, Ching Hua Lee, Ronny Thomale, Xiao-Liang Qi, and Thomas P. Devereaux, “Position-Momentum Duality and Fractional Quantum Hall Effect in Chern Insulators,” *Physical Review Letters* **114**, 236802 (2015).
- [15] Grigory Tarnopolsky, Alex Jura Kruchkov, and Ashvin Vishwanath, “Origin of Magic Angles in Twisted Bilayer Graphene,” *Physical Review Letters* **122**, 106405 (2019).
- [16] Patrick J. Ledwith, Grigory Tarnopolsky, Eslam Khalaf, and Ashvin Vishwanath, “Fractional Chern insulator states in twisted bilayer graphene: An analytical approach,” *Physical Review Research* **2**, 023237 (2020).
- [17] Bruno Mera and Tomoki Ozawa, “Engineering geometrically flat Chern bands with Fubini-Study Kähler structure,” *Physical Review B* **104**, 115160 (2021).
- [18] Jie Wang, Jennifer Cano, Andrew J. Millis, Zhao Liu, and Bo Yang, “Exact Landau Level Description of Geometry and Interaction in a Flatband,” *Physical Review Letters* **127**, 246403 (2021).
- [19] Bruno Mera and Tomoki Ozawa, “Kähler geometry and Chern insulators: Relations between topology and the quantum metric,” *Physical Review B* **104**, 045104 (2021).
- [20] Patrick J. Ledwith, Ashvin Vishwanath, and Eslam Khalaf, “Family of ideal Chern flat bands with arbitrary Chern number in chiral twisted graphene multilayers,” *Physical Review Letters* **128**, 176404 (2022),

- arXiv:2109.11514 [cond-mat].
- [21] Patrick J. Ledwith, Ashvin Vishwanath, and Daniel E. Parker, “Vortexability: A unifying criterion for ideal fractional Chern insulators,” *Physical Review B* **108**, 205144 (2023).
- [22] Manato Fujimoto, Daniel E. Parker, Junkai Dong, Eslam Khalaf, Ashvin Vishwanath, and Patrick Ledwith, “Higher Vortexability: Zero-Field Realization of Higher Landau Levels,” *Physical Review Letters* **134**, 106502 (2025).
- [23] Zhao Liu, Bruno Mera, Manato Fujimoto, Tomoki Ozawa, and Jie Wang, “Theory of Generalized Landau Levels and Implication for non-Abelian States,” *Physical Review X* **15**, 031019 (2025), arXiv:2405.14479 [cond-mat].
- [24] Siddharth A. Parameswaran, Rahul Roy, and Shivaji L. Sondhi, “Fractional quantum Hall physics in topological flat bands,” *Comptes Rendus. Physique* **14**, 816–839 (2013).
- [25] T. S. Jackson, Gunnar Möller, and Rahul Roy, “Geometric stability of topological lattice phases,” *Nature Communications* **6**, 8629 (2015).
- [26] Yan-Qi Li, Yi-Jie Wang, Pei-Han Lin, Bin Wang, and Zhi-Da Song, “Stable Topology in Exactly Flat Bands,” (2026), arXiv:2603.12258 [cond-mat].
- [27] J. E. Avron, R. Seiler, and P. G. Zograf, “Viscosity of Quantum Hall Fluids,” *Physical Review Letters* **75**, 697–700 (1995).
- [28] J. E. Avron, “Odd Viscosity,” *J. Stat. Phys.* **92**, 543 (1998), arXiv:physics/9712050.
- [29] N. Read, “Non-Abelian adiabatic statistics and Hall viscosity in quantum Hall states and $p_x + i p_y$ paired superfluids,” *Physical Review B* **79**, 045308 (2009).
- [30] N. Read and E. H. Rezayi, “Hall viscosity, orbital spin, and geometry: Paired superfluids and quantum Hall systems,” *Physical Review B* **84**, 085316 (2011).
- [31] Carolina Paiva, Jie Wang, Tomoki Ozawa, and Bruno Mera, “Geometrical Responses of Generalized Landau Levels: Structure Factor and the Quantized Hall Viscosity,” (2025), arXiv:2501.11519 [cond-mat].
- [32] A. I. Berdyugin, S. G. Xu, F. M. D. Pellegrino, R. Krishna Kumar, A. Principi, I. Torre, M. Ben Shalom, T. Taniguchi, K. Watanabe, I. V. Grigorieva, M. Polini, A. K. Geim, and D. A. Bandurin, “Measuring Hall viscosity of graphene’s electron fluid,” *Science* **364**, 162–165 (2019).
- [33] F. D. M. Haldane, “Geometrical Description of the Fractional Quantum Hall Effect,” *Physical Review Letters* **107**, 116801 (2011).
- [34] F. D. M. Haldane, “Incompressible Quantum Hall fluids as Electric Quadrupole fluids,” (2023), arXiv:2302.12472 [cond-mat].
- [35] Edward Taylor and Mohit Randeria, “Viscosity of strongly interacting quantum fluids: Spectral functions and sum rules,” *Physical Review A* **81**, 053610 (2010).
- [36] Carlos Hoyos and Dam Thanh Son, “Hall Viscosity and Electromagnetic Response,” *Physical Review Letters* **108**, 066805 (2012).
- [37] Barry Bradlyn, Moshe Goldstein, and N. Read, “Kubo formulas for viscosity: Hall viscosity, Ward identities, and the relation with conductivity,” *Physical Review B* **86**, 245309 (2012).
- [38] Biao Huang, “Hall viscosity revealed via density response,” *Physical Review B* **91**, 235101 (2015).
- [39] Luca V. Delacrétaz and Andrey Gromov, “Transport Signatures of the Hall Viscosity,” *Physical Review Letters* **119** (2017), 10.1103/physrevlett.119.226602.
- [40] Francesco M. D. Pellegrino, Iacopo Torre, and Marco Polini, “Nonlocal transport and the Hall viscosity of two-dimensional hydrodynamic electron liquids,” *Physical Review B* **96**, 195401 (2017).
- [41] Thomas Scaffidi, Nabhanila Nandi, Burkhard Schmidt, Andrew P. Mackenzie, and Joel E. Moore, “Hydrodynamic Electron Flow and Hall Viscosity,” *Physical Review Letters* **118**, 226601 (2017).
- [42] J. Zak, “Magnetic Translation Group,” *Physical Review* **134**, A1602–A1606 (1964).
- [43] S. M. Girvin, A. H. MacDonald, and P. M. Platzman, “Magneto-roton theory of collective excitations in the fractional quantum Hall effect,” *Physical Review B* **33**, 2481–2494 (1986).
- [44] M. O. Goerbig, “Electronic Properties of Graphene in a Strong Magnetic Field,” *Reviews of Modern Physics* **83**, 1193–1243 (2011), arXiv:1004.3396 [cond-mat].
- [45] J. P. Provost and G. Vallee, “Riemannian structure on manifolds of quantum states,” *Communications in Mathematical Physics* **76**, 289–301 (1980).
- [46] M V Berry, “Quantal phase factors accompanying adiabatic changes,” .
- [47] Barry Simon, “Holonomy, the Quantum Adiabatic Theorem, and Berry’s Phase,” *Physical Review Letters* **51**, 2167–2170 (1983).
- [48] F Wilczek and A Shapere, *Geometric Phases in Physics*, Advanced Series in Mathematical Physics, Vol. 5 (WORLD SCIENTIFIC, 1989).
- [49] Shunji Matsuura and Shinsei Ryu, “Momentum space metric, nonlocal operator, and topological insulators,” *Physical Review B* **82**, 245113 (2010).
- [50] Tomoki Ozawa and Bruno Mera, “Relations between topology and the quantum metric for Chern insulators,” *Physical Review B* **104**, 045103 (2021).
- [51] Etienne Guyon, Jean-Pierre Hulin, Luc Petit, and Catalin D. Mitescu, *Physical Hydrodynamics*, 2nd ed. (Oxford university press, Oxford, 2015).
- [52] R. Kubo, “Statistical-Mechanical Theory of Irreversible Processes I - General Theory and Simple Applications to magnetic and Conduction Problems,” *J. Phys. Soc. Jpn.* **12**, 570–586 (1957).
- [53] D. A. Greenwood, “The Boltzmann Equation in the Theory of Electrical Conduction in Metals,” *Proceedings of the Physical Society* **71**, 585–596 (1958).
- [54] See Supplemental Material Sec. I for a detailed derivation.
- [55] I. V. Tokatly and G. Vignale, “New Collective Mode in the Fractional Quantum Hall Liquid,” *Physical Review Letters* **98**, 026805 (2007).
- [56] Claudio Aversa and J. E. Sipe, “Nonlinear optical susceptibilities of semiconductors: Results with a length-gauge analysis,” *Physical Review B* **52**, 14636–14645 (1995).
- [57] Pranav Rao and Barry Bradlyn, “Hall Viscosity in Quantum Systems with Discrete Symmetry: Point Group and Lattice Anisotropy,” *Physical Review X* **10** (2020), 10.1103/physrevx.10.021005.
- [58] In previous work [57], Hall viscosity was expanded in a wedge-product basis. We show in the Supplemental Material that this basis is consistent with Eq. (6).
- [59] Ganesh Sundaram and Qian Niu, “Wave-packet dynamics in slowly perturbed crystals: Gradient corrections and

- Berry-phase effects,” *Physical Review B* **59**, 14915–14925 (1999).
- [60] Di Xiao, Ming-Che Chang, and Qian Niu, “Berry phase effects on electronic properties,” *Reviews of Modern Physics* **82**, 1959–2007 (2010).
- [61] Matthew F. Lapa and Taylor L. Hughes, “Semi-classical wave packet dynamics in non-uniform electric fields,” *Physical Review B* **99**, 121111 (2019), arXiv:1812.10497 [cond-mat].
- [62] Vladyslav Kozii, Alexander Avdoshkin, Shudan Zhong, and Joel E. Moore, “Intrinsic Anomalous Hall Conductivity in a Nonuniform Electric Field,” *Physical Review Letters* **126**, 156602 (2021).
- [63] Thomas I. Tügel and Taylor L. Hughes, “Hall viscosity and momentum transport in lattice and continuum models of the integer quantum Hall effect in strong magnetic fields,” *Physical Review B* **92**, 165127 (2015).
- [64] Taro Kimura, “Hall and spin Hall viscosity ratio in 2d topological insulators,” *Journal of the Physical Society of Japan* **90**, 064705 (2021), arXiv:1004.2688 [cond-mat].
- [65] I. V. Tokatly and G. Vignale, “Lorentz shear modulus of fractional quantum Hall states,” (2008), arXiv:0812.4331 [cond-mat].
- [66] Mohammad Sherafati, Alessandro Principi, and Giovanni Vignale, “Hall viscosity and electromagnetic response of electrons in graphene,” *Phys. Rev. B* **94** (2016), 10.1103/PhysRevB.94.125427.
- [67] Nicola Marzari and David Vanderbilt, “Maximally localized generalized Wannier functions for composite energy bands,” *Physical Review B* **56**, 12847–12865 (1997).
- [68] Nicola Marzari, Arash A. Mostofi, Jonathan R. Yates, Ivo Souza, and David Vanderbilt, “Maximally localized Wannier functions: Theory and applications,” *Reviews of Modern Physics* **84**, 1419–1475 (2012).
- [69] Xing-Lei Ma, Jin-Xin Hu, and K. T. Law, “Universal Boundary-Modes Localization from Quantum Metric Length,” (2025), arXiv:2509.05114 [cond-mat].
- [70] See Supplemental Material for the model Hamiltonians, parameters, numerical evaluations of C , F_Ω , and R used in Fig. 2.
- [71] Hakan Atakışi and M. Ö. Oktel, “Landau levels in lattices with long-range hopping,” *Physical Review A* **88**, 033612 (2013).
- [72] Xiao-Liang Qi, Yong-Shi Wu, and Shou-Cheng Zhang, “Topological quantization of the spin Hall effect in two-dimensional paramagnetic semiconductors,” *Phys. Rev. B* **74**, 085308 (2006).
- [73] F. D. M. Haldane, ““Hall viscosity” and intrinsic metric of incompressible fractional Hall fluids,” (2009), arXiv:0906.1854 [cond-mat].
- [74] Xiao-Liang Qi, Yong-Shi Wu, and Shou-Cheng Zhang, “Topological quantization of the spin Hall effect in two-dimensional paramagnetic semiconductors,” *Physical Review B* **74**, 085308 (2006).

Supplemental Material for “Quantum Geometric Origin of Hall Viscosity and Nonlocal Hall Conductivity in Lattice Bands”

KUBO FORMULA FOR HALL VISCOSITY

We consider the response of the system to a weak, time-dependent strain deformation field. The corresponding perturbation Hamiltonian can be written as^[37]

$$H' = -\dot{\lambda}_{\mu\nu}\hat{J}_{\mu\nu} \quad (\text{S1})$$

in the “velocity” gauge, or equivalently as $H' = -\lambda_{\mu\nu}\hat{T}_{\mu\nu}$ in the “length” gauge. Here, $\lambda_{\mu\nu}$ is the strain deformation tensor and $\dot{\lambda}_{\mu\nu} = \partial_t\lambda_{\mu\nu}$ is the strain rate. The operator $\hat{J}_{\mu\nu}$ generates the strain deformation, and the stress tensor operator is defined by its time derivative, $\hat{T}_{\mu\nu} \equiv -\partial_t\hat{J}_{\mu\nu} = (i/\hbar)[\hat{J}_{\mu\nu}, \hat{H}]$. The viscosity tensor $\eta_{\mu\nu\alpha\beta}$ is defined as the linear response of $\hat{T}_{\mu\nu}$ to $\dot{\lambda}_{\alpha\beta}$,

$$\langle \hat{T}_{\mu\nu} \rangle = -\eta_{\mu\nu\alpha\beta} \frac{\partial \lambda_{\alpha\beta}}{\partial t} \quad (\text{S2})$$

For viscosity, the “velocity” gauge in Eq. (S1) is convenient because the external perturbation couples directly to the strain rate $\dot{\lambda}_{\mu\nu}$. Treating $\dot{\lambda}_{\alpha\beta}(t)$ as the driving force in standard linear-response theory, the time-domain viscosity tensor is^[52, 53]

$$\eta_{\mu\nu\alpha\beta}(t-t') = -\frac{i}{\hbar}\theta(t-t')\langle [\hat{T}_{\mu\nu}(t), \hat{J}_{\alpha\beta}(t')] \rangle_0 \quad (\text{S3})$$

where $\langle \dots \rangle_0$ denotes the expectation value in the unperturbed ground state, and the Heaviside step function $\theta(t-t')$ enforces causality. In the frequency domain,

$$\eta_{\mu\nu\alpha\beta}(\omega) = -\frac{i}{\hbar} \int_0^\infty dt e^{i\omega^+ t} \langle [\hat{T}_{\mu\nu}(t), \hat{J}_{\alpha\beta}(0)] \rangle_0 \quad (\text{S4})$$

where $\omega^+ \equiv \omega + i0^+$ includes an infinitesimal positive imaginary part for adiabatic switching and convergence at $t \rightarrow \infty$. Substituting $\hat{T}_{\mu\nu}(t) = -\partial_t\hat{J}_{\mu\nu}(t)$ and integrating by parts with respect to t yields

$$\begin{aligned} \eta_{\mu\nu\alpha\beta}(\omega) &= \frac{i}{\hbar} \left[e^{i\omega^+ t} \langle [\hat{J}_{\mu\nu}(t), \hat{J}_{\alpha\beta}(0)] \rangle_0 \right]_0^\infty - \frac{i}{\hbar} (i\omega^+) \int_0^\infty dt e^{i\omega^+ t} \langle [\hat{J}_{\mu\nu}(t), \hat{J}_{\alpha\beta}(0)] \rangle_0 \\ &= -\frac{i}{\hbar} \langle [\hat{J}_{\mu\nu}(0), \hat{J}_{\alpha\beta}(0)] \rangle_0 + \frac{\omega^+}{\hbar} \int_0^\infty dt e^{i\omega^+ t} \langle [\hat{J}_{\mu\nu}(t), \hat{J}_{\alpha\beta}(0)] \rangle_0 \end{aligned} \quad (\text{S5})$$

The boundary term vanishes at $t \rightarrow \infty$, whereas the lower boundary at $t = 0$ yields an equal-time commutator. The static Hall viscosity describes the dissipationless response in the dc limit. For a gapped system, the integral in the second term remains finite, and the second term vanishes as $\omega \rightarrow 0$. The remaining contribution is the equal-time contact term, Eq. (3) of the main text.

CONSTRUCTION OF STRAIN DEFORMATION IN LATTICE SYSTEM

Upon projection onto an isolated single band, the effective position operator acquires a covariant form in momentum space, defined as $\hat{X}_\mu = i\nabla_\mu + A_\mu(\mathbf{k})$, where $A_\mu(\mathbf{k}) = i\langle u(\mathbf{k}) | \nabla_\mu | u(\mathbf{k}) \rangle$ denotes the Berry connection. This momentum-space covariant derivative inherently leads to a non-trivial commutation relation between the spatial coordinates:

$$[\hat{X}_\mu, \hat{X}_\nu] = i\Omega_{\mu\nu}(\mathbf{k}), \quad (\text{S6})$$

where $\Omega_{\mu\nu} \equiv \epsilon_{\mu\nu}\Omega = \partial_\mu A_\nu - \partial_\nu A_\mu$ represents the gauge-invariant Berry curvature. We proceed to define the intrinsic electric quadrupole moment operator as $\hat{Q}_{\mu\nu} \equiv \frac{1}{2}\{\hat{X}_\mu, \hat{X}_\nu\} - \langle \hat{X}_\mu \rangle \langle \hat{X}_\nu \rangle$. Here, the disconnected product of expectation

values is explicitly subtracted to isolate the intrinsic spatial variance, ensuring that the defined quadrupole moment behaves as a proper intensive physical quantity. By directly evaluating the commutators using Eq.(S6), one finds that these quadrupolar operators mathematically close the $SO(2,1)$ Lie algebra:

$$[\hat{Q}_{\mu\nu}, \hat{Q}_{\alpha\beta}] = i\Omega_{\nu\beta}\hat{Q}_{\mu\alpha} + i\Omega_{\mu\beta}\hat{Q}_{\alpha\nu} + (\alpha \leftrightarrow \beta). \quad (\text{S7})$$

Equipped with this underlying algebraic structure, we can explicitly construct the strain generator $\hat{J}_{\mu\nu}$ in terms of the quadrupolar components:[34, 73]

$$\hat{J}_{\mu\nu} = \frac{\hbar}{2\Omega}\epsilon_{\nu\lambda}\hat{Q}_{\mu\lambda} + \frac{1}{2}\delta_{\mu\nu}\hat{D}. \quad (\text{S8})$$

It is straightforward to verify that this construction strictly satisfies the fundamental commutation relation for geometric spatial deformations, $[\hat{J}_{\mu\nu}, \hat{X}_\alpha] = i\hbar\hat{X}_\mu\delta_{\alpha\nu}$, provided that the trace component \hat{D} functions as the canonical dilation operator satisfying $[\hat{D}, \hat{X}_\mu] = i\hbar\hat{X}_\mu$. Crucially, the explicit inverse dependence on Ω in Eq. (S8) formally necessitates the fundamental assumption that the Berry curvature is strictly non-vanishing ($\Omega \neq 0$) throughout the Brillouin zone. We emphasize that this topological requirement is significantly broader than the stringent ideal band limit.[23] While a non-vanishing Ω is indeed naturally guaranteed under the stronger geometric condition of saturating the quantum metric bounds, our algebraic construction here places no restrictive constraints on the eigenvalues or the trace of the quantum metric. Consequently, this quadrupolar formalism remains robustly applicable to generic topological bands characterized by a definite-sign Berry curvature, independent of any further ideal geometric structures.

To establish the full algebraic structure of the geometric deformations, we evaluate the commutator of the strain generators $\hat{J}_{\mu\nu}$:

$$[\hat{J}_{\mu\nu}, \hat{J}_{\alpha\beta}] = \frac{\hbar^2}{4\Omega^2} [\epsilon_{\nu\lambda}\hat{Q}_{\mu\lambda}, \epsilon_{\beta\gamma}\hat{Q}_{\alpha\gamma}] - \frac{\hbar}{4\Omega} (\delta_{\mu\nu}[\hat{D}, \epsilon_{\beta\gamma}\hat{Q}_{\alpha\gamma}] + \delta_{\alpha\beta}[\epsilon_{\nu\lambda}\hat{Q}_{\mu\lambda}, \hat{D}]). \quad (\text{S9})$$

Utilizing the canonical dilation commutator $[\hat{D}, \hat{Q}_{\mu\nu}] = 2i\hbar\hat{Q}_{\mu\nu}$, the latter two terms in Eq. (S9) immediately simplify to $i\hbar(\delta_{\mu\nu}\hat{J}_{\alpha\beta} - \delta_{\alpha\beta}\hat{J}_{\mu\nu})$. To evaluate the remaining first term, we substitute the $SO(2,1)$ algebraic relation from Eq. (S7), yielding:

$$\begin{aligned} [\epsilon_{\nu\lambda}\hat{Q}_{\mu\lambda}, \epsilon_{\beta\gamma}\hat{Q}_{\alpha\gamma}] &= i\epsilon_{\nu\lambda}\epsilon_{\beta\gamma}[\hat{Q}_{\alpha\mu}\epsilon_{\lambda\gamma} + \hat{Q}_{\alpha\lambda}\epsilon_{\mu\gamma} + \hat{Q}_{\gamma\mu}\epsilon_{\lambda\alpha} + \hat{Q}_{\gamma\lambda}\epsilon_{\mu\alpha}] \\ &= i[\epsilon_{\nu\lambda}\delta_{\mu\beta}\hat{Q}_{\alpha\lambda} - \epsilon_{\beta\gamma}\delta_{\alpha\nu}\hat{Q}_{\gamma\mu}] + i[\epsilon_{\nu\beta}\hat{Q}_{\alpha\mu} - \epsilon_{\mu\alpha}(\hat{Q}_{\nu\beta} - \delta_{\nu\beta}\hat{Q}_{\gamma\gamma})], \end{aligned} \quad (\text{S10})$$

This expression can be systematically recast in terms of the strain generator $\hat{J}_{\mu\nu}$. Specifically, the first bracketed term in Eq. (S10) reduces to:

$$\epsilon_{\nu\lambda}\delta_{\mu\beta}\hat{Q}_{\alpha\lambda} - \epsilon_{\beta\gamma}\delta_{\alpha\nu}\hat{Q}_{\gamma\mu} = -\frac{2\Omega}{\hbar}(\delta_{\mu\beta}\hat{J}_{\alpha\nu} - \delta_{\alpha\nu}\hat{J}_{\mu\beta}), \quad (\text{S11})$$

which is rigorously derived via the tensor contraction $-\hbar^{-1}\epsilon_{\nu\lambda}\hat{Q}_{\mu\lambda} = 2\Omega(\hat{J}_{\mu\nu} - \delta_{\mu\nu}\hat{D}/2)/\hbar^2$. To simplify the second bracketed term in Eq. (S10), we invert the relation defined in Eq. (S8) to express the quadrupole operators as:

$$\begin{aligned} \frac{\hbar}{2\Omega}\hat{Q}_{\mu\nu} &= \epsilon_{\mu\lambda}\hat{J}_{\nu\lambda} - \frac{1}{2}\epsilon_{\mu\nu}\hat{D} \\ \frac{\hbar}{2\Omega}(\hat{Q}_{\mu\nu} - \delta_{\mu\nu}\hat{Q}_{\gamma\gamma}) &= \epsilon_{\mu\lambda}\hat{J}_{\lambda\nu} - \frac{1}{2}\epsilon_{\mu\nu}\hat{D}. \end{aligned} \quad (\text{S12})$$

This exact inversion directly provides the necessary tensorial components:

$$\begin{aligned} \epsilon_{\nu\beta}\hat{Q}_{\alpha\mu} &= -\frac{2\Omega}{\hbar}(\delta_{\mu\beta}\hat{J}_{\alpha\nu} - \delta_{\mu\nu}\hat{J}_{\alpha\beta} + \frac{1}{2}\epsilon_{\nu\beta}\epsilon_{\mu\alpha}\hat{D}) \\ \epsilon_{\mu\alpha}(\hat{Q}_{\nu\beta} - \delta_{\nu\beta}\hat{Q}_{\gamma\gamma}) &= -\frac{2\Omega}{\hbar}(\delta_{\alpha\nu}\hat{J}_{\mu\beta} - \delta_{\mu\nu}\hat{J}_{\alpha\beta} + \frac{1}{2}\epsilon_{\mu\alpha}\epsilon_{\nu\beta}\hat{D}). \end{aligned} \quad (\text{S13})$$

Finally, substituting the simplified components from Eq. (S11) and Eq. (S13) back into the expanded commutator in Eq. (S9) and Eq. (S10), we arrive at the closed commutation relation for the strain generators:

$$[\hat{J}_{\mu\nu}, \hat{J}_{\alpha\beta}] = -i\hbar(\delta_{\mu\beta}\hat{J}_{\alpha\nu} - \delta_{\nu\alpha}\hat{J}_{\mu\beta}) + i\hbar(\delta_{\mu\nu}\hat{J}_{\alpha\beta} - \delta_{\alpha\beta}\hat{J}_{\mu\nu}). \quad (\text{S14})$$

HALL VISCOSITY IN ANISOTROPIC SYSTEM

To rigorously benchmark our formalism, we must demonstrate that our derived Hall viscosity tensor is completely equivalent to the six-component structure previously identified in the literature.[57] Mathematically, the allowed forms of the Hall viscosity merely represent different choices of basis spanning the specific subspace of antisymmetric rank-four tensors in two dimensions. For a continuous, rotationally invariant system, this tensor space reduces to a single independent component, taking the familiar isotropic form:

$$\eta_{\mu\nu\alpha\beta} = \eta^H(\epsilon_{\mu\beta}\delta_{\nu\alpha} + \epsilon_{\nu\alpha}\delta_{\mu\beta}). \quad (\text{S15})$$

However, when continuous rotational symmetry is broken by an anisotropic crystalline lattice, the tensor space expands to accommodate six independent components. As shown in Ref. [57], this general anisotropic Hall viscosity can be expanded using an explicit tensor basis constructed from the wedge products of Pauli matrices and the Levi-Civita symbol:

$$\begin{aligned} \eta_{\mu\nu\alpha\beta} = & \eta^H(\sigma^z \wedge \sigma^x)_{\mu\nu\alpha\beta} + \gamma(\sigma^z \wedge \epsilon)_{\mu\nu\alpha\beta} + \Theta(\sigma^x \wedge \epsilon)_{\mu\nu\alpha\beta} \\ & \bar{\eta}^H(\delta \wedge \epsilon)_{\mu\nu\alpha\beta} + \bar{\gamma}(\delta \wedge \sigma^x)_{\mu\nu\alpha\beta} + \bar{\Theta}(\sigma^z \wedge \delta)_{\mu\nu\alpha\beta}, \end{aligned} \quad (\text{S16})$$

where the wedge product is defined as $(A \wedge B)_{\mu\nu\alpha\beta} = A_{\mu\nu}B_{\alpha\beta} - A_{\alpha\beta}B_{\mu\nu}$. In contrast, our microscopic quadrupolar formulation yields a remarkably compact expression dictated by the strain generator $J_{\mu\nu}$:

$$\begin{aligned} \eta_{\mu\nu\alpha\beta} = & \delta_{\mu\beta}J_{\alpha\nu} - \delta_{\nu\alpha}J_{\mu\beta} \\ & \delta_{\alpha\beta}J_{\mu\nu} - \delta_{\mu\nu}J_{\alpha\beta}. \end{aligned} \quad (\text{S17})$$

Since the strain generator $J_{\mu\nu}$ can be generally decomposed into a linear combination of the 2D matrices ϵ , σ^x , and σ^z , our expression in Eq. (S17) fundamentally lives in the exact same tensor subspace as Eq. (S16) and the apparent mathematical difference is merely a change of tensor basis. While it is straightforward that the second line of Eq. (S17) is consistent with that of Eq. (S16), it suffices to show this also applies to the first line. Without loss of generality, we examine the fundamental building block of the isotropic Hall viscosity and establish the following tensor identity:

$$\epsilon_{\mu\beta}\delta_{\nu\alpha} + \epsilon_{\nu\alpha}\delta_{\mu\beta} = \sigma_{\mu\nu}^z\sigma_{\alpha\beta}^x - \sigma_{\mu\nu}^x\sigma_{\alpha\beta}^z. \quad (\text{S18})$$

To verify this identity explicitly, we construct an orthonormal Cartesian basis in two dimensions, denoted by vectors $X = (1, 0)^T$ and $Y = (0, 1)^T$. The constituent tensors can be explicitly expressed via outer products:

$$\delta_{\mu\nu} = X_\mu X_\nu + Y_\mu Y_\nu \quad \epsilon_{\mu\nu} = X_\mu Y_\nu - X_\nu Y_\mu \quad \sigma_{\mu\nu}^x = X_\mu Y_\nu + X_\nu Y_\mu \quad \sigma_{\mu\nu}^z = X_\mu X_\nu - Y_\mu Y_\nu. \quad (\text{S19})$$

By substituting these representations into both sides of Eq. (S18), a direct algebraic expansion of the left-hand side yields:

$$\begin{aligned} \epsilon_{\mu\beta}\delta_{\nu\alpha} + \epsilon_{\nu\alpha}\delta_{\mu\beta} = & (X_\mu Y_\beta - X_\beta Y_\mu)(X_\nu X_\alpha + Y_\nu Y_\alpha) + (X_\nu Y_\alpha - X_\alpha Y_\nu)(X_\mu X_\beta + Y_\mu Y_\beta) \\ = & X_\mu Y_\beta X_\nu X_\alpha + X_\mu Y_\beta Y_\nu Y_\alpha - X_\beta Y_\mu X_\nu X_\alpha - X_\beta Y_\mu Y_\nu Y_\alpha + (\mu \leftrightarrow \nu, \alpha \leftrightarrow \beta). \end{aligned} \quad (\text{S20})$$

Similarly, evaluating the right-hand side constructed from the Pauli matrices gives:

$$\begin{aligned} \sigma_{\mu\nu}^z\sigma_{\alpha\beta}^x - \sigma_{\mu\nu}^x\sigma_{\alpha\beta}^z = & (X_\mu X_\nu - Y_\mu Y_\nu)(X_\alpha Y_\beta + X_\beta Y_\alpha) - (X_\mu Y_\nu + X_\nu Y_\mu)(X_\alpha X_\beta - Y_\alpha Y_\beta) \\ = & X_\mu X_\nu X_\alpha Y_\beta + X_\mu X_\nu X_\beta Y_\alpha - Y_\mu Y_\nu X_\alpha Y_\beta - Y_\mu Y_\nu X_\beta Y_\alpha - (\mu \leftrightarrow \alpha, \nu \leftrightarrow \beta). \end{aligned} \quad (\text{S21})$$

Comparing Eq. (S20) and Eq. (S21) strictly verifies the identity in Eq.(S18). Extending this algebraic matching to the remaining anisotropic terms straightforwardly proves that our compact formulation in Eq.(S17) is an exact, basis-independent equivalent of the general six-component tensor described in Eq. (S16).

MODEL CALCULATIONS FOR FIG. 1 OF THE MAIN TEXT

In this section, we describe the model calculations used to obtain the nonlocal Hall ratio R and the Berry-curvature fluctuations F_Ω shown in Fig. 1 of the main text. We therefore focus on the Berry curvature, the quantum metric, and the violation of the trace condition, rather than on the band dispersion. For each model, we diagonalize the single-particle Hamiltonian on a uniform $N_k \times N_k$ mesh in the Brillouin zone and select an isolated Chern band.

Projector formulation of band geometry

For the numerical calculations of the band geometry, we use the gauge-invariant projector representation. For the isolated target band, we introduce the band projector

$$\mathcal{P}(\mathbf{k}) = |u(\mathbf{k})\rangle \langle u(\mathbf{k})|, \quad (\text{S22})$$

where $|u(\mathbf{k})\rangle$ is the cell-periodic Bloch eigenstate of the target band. The quantum metric and Berry curvature are defined by

$$g_{\mu\nu}(\mathbf{k}) = \frac{1}{2} \text{Tr}[\partial_\mu \mathcal{P}(\mathbf{k}) \partial_\nu \mathcal{P}(\mathbf{k})], \quad (\text{S23})$$

$$\Omega_{\mu\nu}(\mathbf{k}) = -i \text{Tr} \{ \mathcal{P}(\mathbf{k}) [\partial_\mu \mathcal{P}(\mathbf{k}), \partial_\nu \mathcal{P}(\mathbf{k})] \}, \quad (\text{S24})$$

with $\Omega(\mathbf{k}) = \Omega_{xy}(\mathbf{k})$, following the same sign convention of the main text. The partial derivatives of $\mathcal{P}(\mathbf{k})$ are evaluated by central finite differences with periodic boundary conditions in the Brillouin zone. The Chern number is also checked using a gauge-invariant link-variable discretization.

Qi–Wu–Zhang model

As a generic nonideal Chern-band model, we use the two-band Qi–Wu–Zhang (QWZ) Hamiltonian [74],

$$H_{\text{QWZ}}(\mathbf{k}) = \sin k_x \sigma_x + \sin k_y \sigma_y + (m + \cos k_x + \cos k_y) \sigma_z. \quad (\text{S25})$$

The parameter m is chosen in the Chern-insulating regime. In Fig. S1, we have used $m = -1$ and $N_k = 401$. The Brillouin zone is $(k_x, k_y) \in [-\pi, \pi)^2$. After diagonalizing $H_{\text{QWZ}}(\mathbf{k})$, we compute $g_{\mu\nu}(\mathbf{k})$, $\Omega(\mathbf{k})$, F_Ω , and R from the formulas given above. For this model, both the Berry curvature and the quantum metric vary strongly over the Brillouin zone, and the trace condition is not generally satisfied. This makes the QWZ model a useful representative of a generic nonideal Chern band.

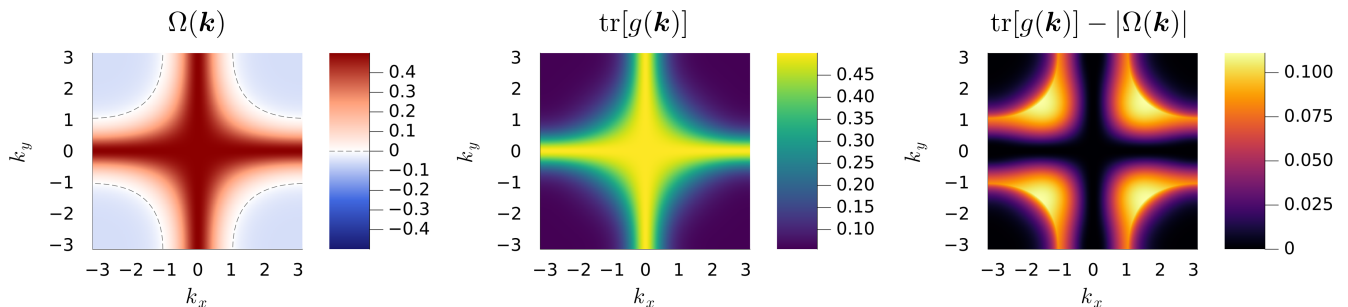


FIG. S1. Brillouin-zone distributions of $\Omega(\mathbf{k})$, $\text{tr}[g(\mathbf{k})]$, and $\text{tr}[g(\mathbf{k})] - |\Omega(\mathbf{k})|$ for the QWZ model. The gray dashed contour in the left panel indicates $\Omega(\mathbf{k}) = 0$.

Kapit–Mueller model

As a nearly Landau-level reference, we use the Kapit–Mueller (KM) model on a square lattice with complex long-range hopping [71]. Lattice sites are labeled by integer coordinates (x_j, y_j) . The Hamiltonian is given by

$$H_{\text{KM}} = \sum_{j \neq k} J_{jk} c_j^\dagger c_k, \quad (\text{S26})$$

where

$$J_{jk} = (-1)^{\Delta x + \Delta y + \Delta x \Delta y} \exp \left[-\frac{\pi}{2} (1 - \phi) (\Delta x^2 + \Delta y^2) \right] \exp [i\pi \phi (x_j + x_k) \Delta y], \quad (\text{S27})$$

with $\Delta x = x_k - x_j$ and $\Delta y = y_k - y_j$. Here, $\phi = p/q$ is the magnetic flux per plaquette. For rational flux, magnetic translation symmetry enlarges the unit cell to q sites, and the Hamiltonian is reduced to a $q \times q$ Bloch Hamiltonian in the corresponding magnetic Brillouin zone. We take the flat Chern band as the target band. The parameters used for Fig. S2 are $\phi = 1/4$ and $N_k = 301$. In the numerical calculation, the long-range hopping is truncated at $|\Delta x|, |\Delta y| \leq 6$. For these parameters, the Berry curvature is weakly nonuniform, while the trace condition is well satisfied. Thus, the KM model provides a lattice realization close to the continuum Landau-level limit, with a small residual Berry-curvature fluctuation.

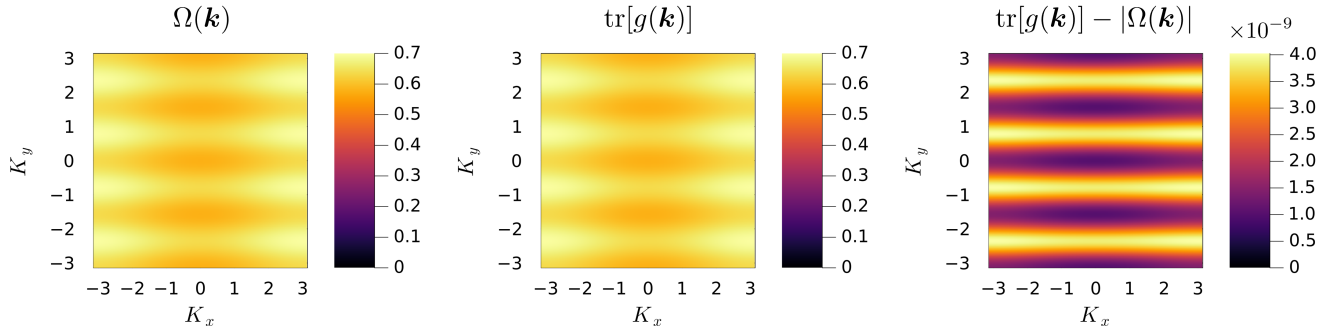


FIG. S2. Magnetic-Brillouin-zone distributions of $\Omega(\mathbf{k})$, $\text{tr}[g(\mathbf{k})]$, and $\text{tr}[g(\mathbf{k})] - |\Omega(\mathbf{k})|$ for the KM model. The maps are plotted as functions of the magnetic Bloch wave vectors (K_x, K_y) , while the geometric quantities are evaluated in the physical wave vectors $k_x = K_x/q$ and $k_y = K_y$.

Chiral twisted bilayer graphene

As a moiré Chern-band example, we use the chiral limit of the continuum model for twisted bilayer graphene (chiral TBG) [15, 16]. For a single valley, the continuum Hamiltonian is written as

$$H_{\text{TBG}} = \begin{pmatrix} h_{+\theta/2}(-i\nabla) & T(\mathbf{r}) \\ T^\dagger(\mathbf{r}) & h_{-\theta/2}(-i\nabla) \end{pmatrix}, \quad (\text{S28})$$

where h_θ is the rotated Dirac Hamiltonian

$$h_\theta(-i\nabla) = -\hbar v_F [R_\theta(-i\nabla)] \cdot (\sigma_x, \sigma_y), \quad R_\theta = \begin{pmatrix} \cos \theta & \sin \theta \\ -\sin \theta & \cos \theta \end{pmatrix}, \quad (\text{S29})$$

with v_F the Fermi velocity of monolayer graphene. The moiré tunneling matrix is

$$T(\mathbf{r}) = \sum_{j=1}^3 T_j e^{-i\mathbf{q}_j \cdot \mathbf{r}}, \quad T_j = w_0 \sigma_0 + w_1 \left[\cos \frac{2\pi(j-1)}{3} \sigma_x + \sin \frac{2\pi(j-1)}{3} \sigma_y \right]. \quad (\text{S30})$$

The chiral limit is defined by $w_0 = 0$, while $w_1 \neq 0$. We parametrize the model by the dimensionless coupling

$$\alpha = \frac{w_1}{\hbar v_F k_\theta}, \quad (\text{S31})$$

where k_θ is the moiré wave-vector scale. We set the momentum transfers as $\mathbf{q}_1 = k_\theta(0, -1)$ and $\mathbf{q}_{2,3} = k_\theta(\pm\sqrt{3}/2, 1/2)$, and the moiré reciprocal lattice vectors as $\mathbf{b}_{1,2} = k_\theta(\pm\sqrt{3}/2, 3/2)$. The Hamiltonian is diagonalized in a plane-wave basis $\mathbf{k} + \mathbf{G}$, where $\mathbf{G} = n_1 \mathbf{b}_1 + n_2 \mathbf{b}_2$. This basis is truncated by the hexagonal shell condition $\max\{|n_1|, |n_2|, |n_1 + n_2|\} \leq N_{\text{shell}}$. The parameters used for Fig. S3 are $N_{\text{shell}} = 4$, $N_k = 301$, and $\alpha = 0.586$, close to the first chiral magic angle [15]. We choose the $C = +1$ chiral nearly flat band as the target band. Berry curvature and the quantum metric have similar Brillouin-zone profiles, while $\text{tr}[g(\mathbf{k})] - |\Omega(\mathbf{k})|$ remains very small, indicating that the selected chiral flat band is close to the ideal trace condition.

Numerical summary.— The numerical values used in Fig. 1 of the main text are summarized in Table S1. The KM and chiral TBG results lie close to the ideal band relation $R = 1 + F_\Omega^2$, whereas the QWZ model shows a visible deviation, reflecting the lack of trace condition and strong nonuniformity of Berry curvature.

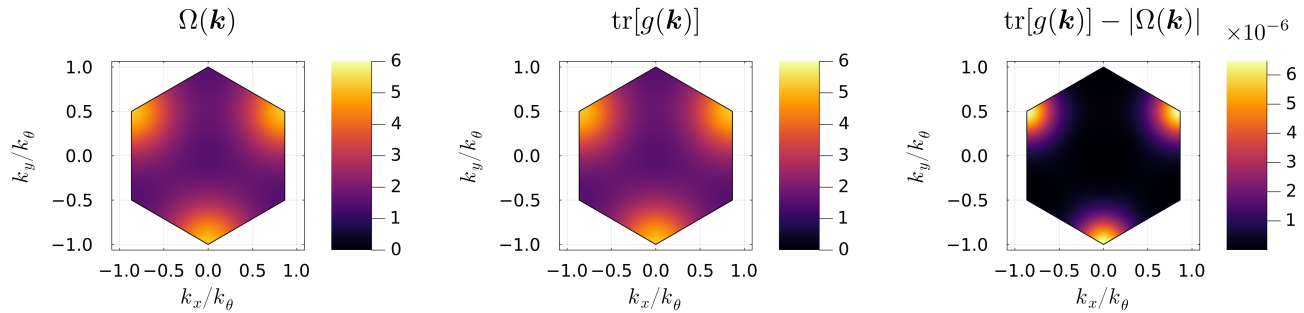


FIG. S3. Brillouin-zone distributions of $\Omega(\mathbf{k})$, $\text{tr}[g(\mathbf{k})]$, and $\text{tr}[g(\mathbf{k})] - |\Omega(\mathbf{k})|$ for the chiral TBG.

TABLE S1. Numerical values used in Fig. 1 of the main text.

Model	Parameters	C	F_Ω	$1 + F_\Omega^2$	R
QWZ	$m = -1$	+1	1.29441	2.67550	2.77512
KM	$\phi = 1/4$	+1	0.04693	1.00220	1.00216
chiral TBG	$\alpha = 0.586$	+1	0.36815	1.13553	1.13553